J Comp Physiol A
DOI 10.1007/s00359-008-0317-3

ORIGINAL PAPER

Image motion environments: background noise for movement-based animal signals

Richard Peters · Jan Hemmi · Jochen Zeil

Received: 17 July 2007 / Revised: 10 January 2008 / Accepted: 19 January 2008

Abstract Understanding the evolution of animal signals has to include consideration of the structure of signal and noise, and the sensory mechanisms that detect the signals. Considerable progress has been made in understanding sounds and colour signals, however, the degree to which movement-based signals are constrained by the particular patterns of environmental image motion is poorly understood. Here we have quantified the image motion generated by wind-blown plants at 12 sites in the coastal habitat of the Australian lizard *Amphibolurus muricatus*. Sampling across different plant communities and meteorological conditions revealed distinct image motion environments. At all locations, image motion became more directional and apparent speed increased as wind speeds increased. The magnitude of these changes and the spatial distribution of image motion, however, varied between locations probably as a function of plant structure and the topographic location. In addition, we show that the background motion noise depends strongly on the particular depth-structure of the environment and argue that such micro-habitat differences suggest specific strategies to preserve signal efficacy. Movement-based signals and motion processing mechanisms, therefore, may reveal the same type of habitat specific structural variation that we see for signals from other modalities.

Keywords Movement-based signal · Image motion · Visual ecology · Signal evolution · Lizard

R. Peters (✉) · J. Hemmi · J. Zeil
Centre for Visual Sciences,
Research School of Biological Sciences,
The Australian National University,
Canberra, ACT 0200, Australia
e-mail: richard.peters@anu.edu.au

J. Hemmi · J. Zeil
Australian Research Council Centre for Excellence in Vision Science, Research School of Biological Sciences,
The Australian National University,
Canberra, ACT 0200, Australia

Introduction

The design of animal signals is influenced by the environment in which they are emitted and by the sensory system of receivers that must detect them [reviewed by Lythgoe (1979); Dusenbery (1992); Bradbury and Vehrencamp (1998)]. For sounds, for instance, habitat specific transmission properties determine the optimal temporal structure of auditory signals (Wiley and Richards 1982), and can lead to within species variation based on geographic location (reviewed in Bradbury and Vehrencamp 1998). Similarly, the divergence in vibrational signals produced by insects can be attributed partly to the transmission properties of the host plant (Cocroft and Rodriguez 2005). Another environmental constraint imposed on effective communication is irrelevant sensory stimulation within the same modality (noise). Variation in the ambient noise spectra across habitats has resulted in call divergence in little greenbuls (*Andropadus virens*) (Slabbekoorn and Smith 2002), while differences in the neural filters of cricket frogs (*Acris crepitans*) reflect the environmental noise characteristics of the habitats they occupy (Witte et al. 2005).

Environmental conditions, however, are variable and so animals may need to adjust their signalling behaviour accordingly (Potash 1972; Cynx et al. 1998; Brumm et al. 2004; Peters et al. 2007). To ensure reliable detection,

calling behaviour can be adjusted to avoid the calls of sympatric congeners (Greenfield 1988), as well as other potential masking sounds including anthropogenic sounds (Slabbekoorn and Peet 2003; Sun and Narins 2005; Slabbekoorn and den Boer-Visser 2006), rain (Lengagne and Slater 2002) and wind (Hayes and Huntly 2005). Meteorological conditions also affect the spectral environment for static visual signals (Endler 1993), which influences lek placement in forest-dwelling birds (Endler and Thery 1996), as well as the image motion environment, leading to changes in movement-based signals (Ord et al. 2007; Peters et al. 2007). Understanding environmental conditions can therefore help to explain why signals vary, particularly within species, and to identify neural processing strategies that are used to detect these signals.

For movement-based visual signalling, the particular patterns of environmental image motion that necessitate motion signal adjustment, however, are poorly understood. Quantifying motion and identifying the perceptual constraints faced by animals that communicate with movement is challenging. Image motion has to be computed by the brain from the temporal and spatial correlations of photoreceptor signals. Although the computational structure of motion perception is well understood, in most animals it is still practically impossible to accurately quantify image motion signals from the animal's perspective under natural conditions. Nevertheless, recent advances in computer vision mean that we can now quantify motion signals in a way that informs us of the constraints involved in the perception of relevant, natural motion signals (Zeil and Zanker 1997; Peters et al. 2002; Boeddeker et al. 2005; Zanker and Zeil 2005; Elias et al. 2006). Quantitative modelling can predict where motion signal detection will be difficult (Peters and Hemmi in preparation), and how signal structure might be made more effective [e.g., Fleishman (1988); Ord et al. (2007)]. It is now possible to address in greater detail the structure of image motion environments that influence the detection of rare but important visual motion events, such as those produced by a signalling animal.

For many animals, the primary source of motion noise for movement-based signals comes from wind blown plants (Fleishman 1986, 1988; Eckert and Zeil 2001). The effect of wind on plant motion at a given site is expected to vary along a variety of dimensions including the physical topography of the site, which influences relative exposure to wind, and the height above ground (Hannah et al. 1995). In addition, the force required to generate movement will vary across plant species because of differences in their shape and mechanical properties [e.g., Wood (1995)]. The combined effects of these and other parameters, in particular, the depth structure of the environment (Fleishman 1986), ensure that image motion due to wind-blown plants will vary considerably in space and time and this spatiotemporal structure will be very hard to predict from first principles. In the present study, we present a comprehensive analysis of selected image motion environments for an Australian lizard, *Amphibolurus muricatus*. These highly territorial agamid lizards use a stereotyped sequence of motor patterns during agonistic encounters (Peters and Ord 2003), which convey information to receivers about the quality of the signaller. The distribution of these lizards includes large populations in coastal reserves (Cogger 1996) that are densely vegetated with shrubs (Costermans 2005). Communicative signals are therefore performed in environments in which variable wind conditions generate irregular patterns of plant motion. Our goal was to sample this image motion variation to quantify the likely processing constraints on signal detection. We build on earlier work on the image motion caused by animal signals and some arbitrarily selected wind-blown plants (Fleishman 1988; Peters and Evans 2003). In contrast to these previous analyses, the current study quantified image motion across 12 known basking sites of lizards, which we could correlate with the prevailing wind conditions that we logged concurrently. Our results demonstrate that the specific temporal and spatial pattern of image motion due to wind blown plants depends on the prevailing wind conditions and the specific microhabitat. We discuss how the depth layout of the environment affects the structure of the image motion noise and what consequences that has for signalling strategies.

Materials and methods

Site selection

Jacky lizards are typically found basking on elevated perches such as small trees and shrubs, fallen branches and rocky outcrops (Fig. 1a). Males defend territories from rivals using stereotyped movement-based displays that must be distinguished from the motion of wind-blown plants. To sample a range of visual motion habitats, we identified the typical perch sites of these lizards. At the start of spring 2005 (September) we surveyed the coastal national parks and reserves of New South Wales, on the east coast of Australia, from Botany Bay National Park in the north to Nadgee Nature Reserve in the south. The plant species that surrounded perch sites varied within a locality but were quite similar from one park to the next. We therefore restricted our study area to 12 sites within a single national park (Murramarang National Park). These sites feature plants that are typical of coastal heath, including native grasses and shrubs

Fig. 1 **a** *Amphibolurus muricatus* can be found basking on small trees and shrubs as well as other elevated perches. The perch site for this male was located 180 cm from the ground in front of a coastal banksia (*Acacia longifolia*) shrub. **b** Photograph showing the recording set-up for site 1, and **c** an exported image from the first session of filming

(Table 1). All of our focal plants represent the background of known basking sites. Some of these plants are also utilised at times for basking (e.g., *Banksia integrifolia*), while others only ever surround perches (e.g., *Spinifex sericeus*).

Recording plant motion

Our goal was to sample plant motion under a range of meteorological conditions, particularly, variations in wind speed. We visited each of the 12 sites seven times from October to December 2005. While videotaping plants we measured in synchrony a range of meteorological variables including wind speed and direction.

Equipment

Digital video of wind-blown plants was recorded using a Canon XM2 mini-DV camcorder (Canon Inc., USA) mounted on a tripod with adjustable head. The camera's exposure was set to a shutter speed of 1/250, with aperture allowed to vary. A Kestrel 4000 weather meter (Nielsen–Kellerman, USA) was used to log wind speed every 2 s. Wind direction was determined using a hand-made windsock and recorded manually.

Filming procedure

All sites were filmed on seven separate occasions to sample variation in meteorological conditions, although the first session was used only to determine the best filming geometry and camera settings. We took measurements and photographs during session 1 to ensure accurate replication of the recording set-up for subsequent sessions at each site. We measured the height of the camera from the ground, its distance from a stationary object like a tree trunk in the field of view, and the distance from the camera to the closest plant (Table 1). Digital photographs of the set-up (Fig. 1b), as well as an exported video-frame (Fig. 1c) from the first session helped to verify that the camera's perspective matched the initial recording. The camera and data loggers were synchronised at the start of each day. We filmed for several minutes on each occasion.

Meteorological conditions

We visited each site at different times of the day and during different climatic conditions (e.g., full sun and overcast). The majority of filming sessions featured plant motion caused by wind blowing from an easterly direction

Table 1 Description of jacky lizard perch sites selected as representative image motion environments

Site	Image frame	Plants common name[a]	Species name	Height[b]	Filming distance[c]
1		Coast banksia	*Banksia integrifolia*	156	150
2		Kangaroo grass	*Poa poiformis*	36	52
3		Mat Rush	*Lomandra longifolia*	115	135
4		(Mixed species)	*(incl. L. longifolia, P. poiformis)*	80	160
5		Coast wattle	*Acacia sophorae*	87	115
6		Hairpin banksia	*Banksia spinulosa*	90	146
7		Coast bearded heath	*Leucopogon parviflorus*	105	162
8		Grey (Swamp) She-Oak	*Casuarina glauca*	72	207
9		Bracken	*Pteridium esculentum*	77	69
10		Spinifex grass	*Spinifex sericeus*	72	67
11		Coast rosemary	*Westringia fruticosa*	52	120
12	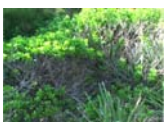	Coastal boobialla	*Myoporum boninense subsp. australe*	80	137

[a] Identification based on Costermans (2005) and Hardwick (2001)

[b] Vertical height of camera from ground (cm)

[c] Distance of camera from nearest foliage (cm)

(median: 80°; Fig. 2a). Taking filming direction into account and projecting wind direction on to the video frame, the majority of sessions featured wind originating from the bottom left or from the left. Wind direction was stable at each site; however, certain sites were prone to stronger winds than others (Fig. 2b).

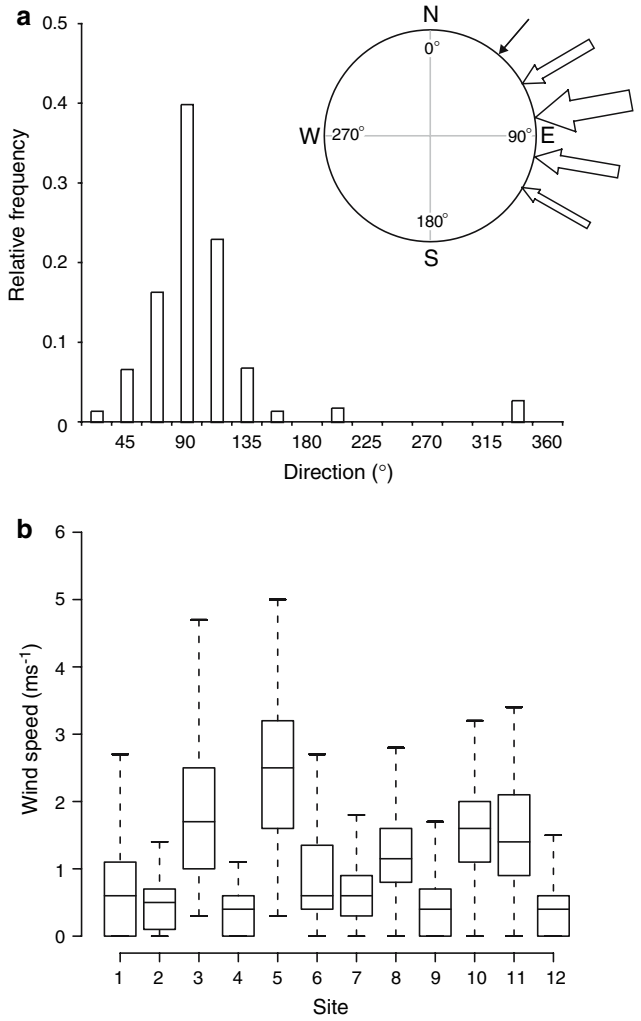

Fig. 2 Plant motion footage was collected under varying wind conditions. **a** Frequency histogram of wind direction in 22.5° bins across all 12 sites and 6 recording sessions (0° represents wind from the north). *Inset*: plot depicting origin of wind during filming. *Arrow width* is proportional to frequency and illustrates that wind blew from an easterly direction (median: 80°) for most filming sessions. **b** Average wind speed by site for all recording sessions, recorded at the focal height of filming. For each site, the *rectangular box* depicts the inter-quartile range and is dissected by the median, while the tails represent the smallest and largest non-outliers ($N = 360$)

Quantifying image motion

We imported video footage of sessions 2–7 directly from tape to an Apple G5 iMac using iMovie HD 5.0.2. Clips were trimmed to two-minute sequences (3,000 frames) and exported as AVI files using the DV/DVCPRO-PAL compressor type (quality set at "best"). These were then transferred to a Toshiba Tecra S2 PC for motion analysis. To avoid frame jitter, we removed the odd video field of input sequences and restored the original frame aspect ratio using bilinear interpolation at 25 frames per second. Video images were down-sampled to 144 × 180 pixels to reduce computational load; spatial averaging is consistent with models of visual processing (Reichardt and Egelhaaf 1988; Egelhaaf et al. 1989). Image motion was quantified using a custom written Matlab program that has been described in detail elsewhere (Peters et al. 2002; Peters and Evans 2003). Briefly, the program is based on a gradient detector model and calculates the velocity field in image sequences based on temporal and spatial derivatives of filtered versions of image intensity [see Peters et al. (2002) and references therein for details]. Image velocities were measured in pixels per second, but were then converted to degrees per second based on the recording distance and the field of view of the camera. To make the recordings from different sites comparable, image velocities were also standardised to a fixed recording distance of 1 m. This was achieved by filming an object of known size positioned at the closest part of each plant, enabling us to calibrate movement amplitudes in mm/s. Knowing the camera distance, we then transformed these values to °/s at a viewing distance of 1 m using the tangent function. All image velocities reported here are therefore measured in °/s as seen by an observer 1 m from the closest part of the plant. Unlike biologically inspired detector models (e.g. Zanker and Zeil 2005), the gradient models measure true velocity independent of image contrast and are therefore less sensitive to prevailing light conditions. The velocity field for a single frame is represented as horizontal and vertical vector components at each spatial location, which can be summarised in scatter plots of velocity (Fig. 3a). The Cartesian representation is converted to polar coordinates describing motion direction and speed. We describe and analyse the velocity field as separate vector components of motion direction and speed. The distribution of motion estimates (Fig. 3a) was summarised using 5 speed bins (Fig. 3b), and 8 directionally selective bins, each spanning 45° (Fig. 3c). Motion speed values were log-transformed. Each direction and speed bin counted the number of estimates that fell within its range of values.

Presentation of data and statistical analysis

We begin by describing the image motion environment at a few sites under different wind conditions to illustrate how the velocity field changes with prevailing winds. We then quantify statistically the effect of wind on the velocity field. However, as the sampling rate of meteorological data (2 s) and image motion (1/25 s) differed, for statistical analysis we averaged across 10 s time windows for each (5 measurements and 250 frames for meteorological data and image motion, respectively) after synchronising the starting point. This resulted in 12 data points for each of the 6 two-minute filming sessions at each site. All statistical analyses were conducted using R 2.3.1 (R Development Core Team 2006).

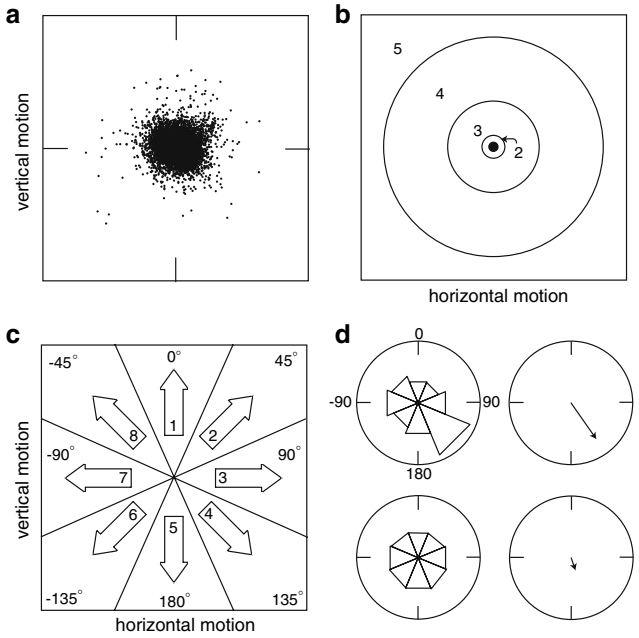

Fig. 3 Our motion analysis results in a measurement of local image velocity (°/s) at each pixel location in the image based on temporal and spatial derivatives of filtered versions of image intensity (see "Materials and methods" for details). **a** The velocity field is represented as horizontal and vertical vector components at each pixel location, which can be summarised in scatter plots (*velocity space*) to show the distribution of motion across the image for each frame interval (40 ms): motion direction is given by its angular position in velocity space relative to the vertical, while the distance from the origin reflects angular speed (°/s). **b** Velocity space was subdivided with concentric circles for sorting angular speed measurements into 5 non-overlapping bins, in log units. Bin *1*: less than −1.5 (0.22°/s; *black dot*). Bin *2*: −1.5 to 0.5 (0.22–1.65°/s). Bin *3*: 0.5 to 1.5 (1.65–4.48°/s). Bin *4*: 1.5 to 2.5 (4.48–12.18°/s). Bin *5*: greater than 2.5 (12.18°/s). **c** To summarise image motion direction, we partitioned velocity space into 8 non-overlapping direction bins each spanning 45°. **d** To determine directionality, we calculated the cumulative distribution of motion vectors in each direction bin for 10 s time intervals, as depicted in rose plots (*left*), and used vector addition to determine the mean vector (*right*). The magnitude (*M*) of the mean vector provides an estimate of the directionality. Values in **a**, **b** and **c** are not constrained to within the bounding box

Motion direction

We considered whether particular directions dominated the image motion caused by plant movements. The direction histograms (Fig. 3c) can be summarised using vector addition (Fig. 3d, left). The resultant vector indicates the average direction, as well as its relative magnitude (*M*). Low values for *M* indicate a relatively even distribution of direction estimates in the original data set; high values reflect a stronger directional component to the motion distribution (Fig. 3d, right). Prior to determining the mean vector, frequencies were converted to relative frequencies (i.e., proportion of estimates within the 10 s time window). Although individual plants, or parts of plants, exhibit rhythmical back-and-forth oscillations, this way of summarising the distribution across the entire field of view, averages over variable and un-synchronised oscillations of plants.

We examined the relationship between wind speed (Ws), site and *M* using the linear model $M = \text{Ws} \times \text{Site}$, testing for different effects of wind speed at each site (LM function in R2.3.1). The statistical significance of the full model (Ws + site + Ws.site), as well as individual model parameters (Ws, site, Ws.site), were tested with the *F* test and checked graphically for outliers and an appropriate error distribution.

Angular speed

Speed bin frequencies had a non-normal distribution and could not be corrected sufficiently with transformation. After visual inspection of the data we deduced that the image motion distribution was skewed by low-level responses very close to zero. In order to conduct formal statistical analysis, we decided to threshold bin frequencies by removing responses close to or equal to zero, thereby allowing us to perform appropriate transformations. The threshold was set at 5% of a given bin's maximum frequency for any 10 s time-window across the full data set. Retaining only the data points that exceeded the threshold, we set up generalised linear models with quasi-poisson error distributions (GLM function in R2.3.1) assessing independently speed bin frequency (*S*) against the predictor variables of wind speed (Ws) and site: $S = \text{Ws} \times \text{Site}$. The statistical significance of individual model parameters were tested with the *F* test.

Distance effects on perceived angular speed

The 3-dimensional nature of the plant environment will influence the speed of perceived image motion (Fleishman 1986). In order to minimize the complicating effects of distance, we filmed sites that, with the exception of site 4, were comprised of single plants with relatively narrow depth structures. Under normal circumstances, however, *A. muricatus* habitats comprise plants at varying distances. In the same way as the angular size of an object depends on viewing distance, angular speed is also distance dependent. An object moving through a distance (x) at a viewing distance (d) moves through an angle (θ) at the eye of an observer:

$$\tan\left(\frac{\theta}{2}\right) = \frac{x}{2d} \quad (1)$$

$$\theta = 2\tan^{-1}\left(\frac{x}{2d}\right) \quad (2)$$

Differentiating (2) with respect to time, we obtain the angular speed $(\dot{\theta})$ of the object depending on the apparent movement amplitude (θ), the distance (d) and the movement speed $(\dot{x})$:

$$\dot{\theta} = \cos^2\left(\frac{\theta}{2}\right)\frac{\dot{x}}{d} \quad (3)$$

For small apparent movement amplitudes, $\theta < 20°$ (which is approximately half the field of view of a standard video camera) Eq. (3) simplifies to

$$\dot{\theta} = \frac{\dot{x}}{d}. \quad (4)$$

To model the effect of viewing distance on angular speeds, we used Eq. (4) to predict the range of angular speeds generated by plant movements of varying speeds as seen from different distances. To simplify the simulations, plant movements were generated by a single plant, and with all parts of the plant moving at the same speed (in cm/s). Viewing distances are reported as mean distances ± 10 cm standard deviations (based on a normal distribution) to simulate the natural depth structure of plants.

Results

Image motion environments

Image motion caused by wind blown plants varies with prevailing wind conditions. To illustrate this general pattern of results we summarise data obtained from site 1 (*Acacia longifolia*) under different wind conditions to show how the velocity distributions change (Fig. 4). In wind-still conditions (Fig. 4a), the distribution of estimates in *velocity space* suggests little detectable image motion. Looking now at motion direction and speed separately, we can see an even distribution of motion direction estimates in the *direction profile*, while the

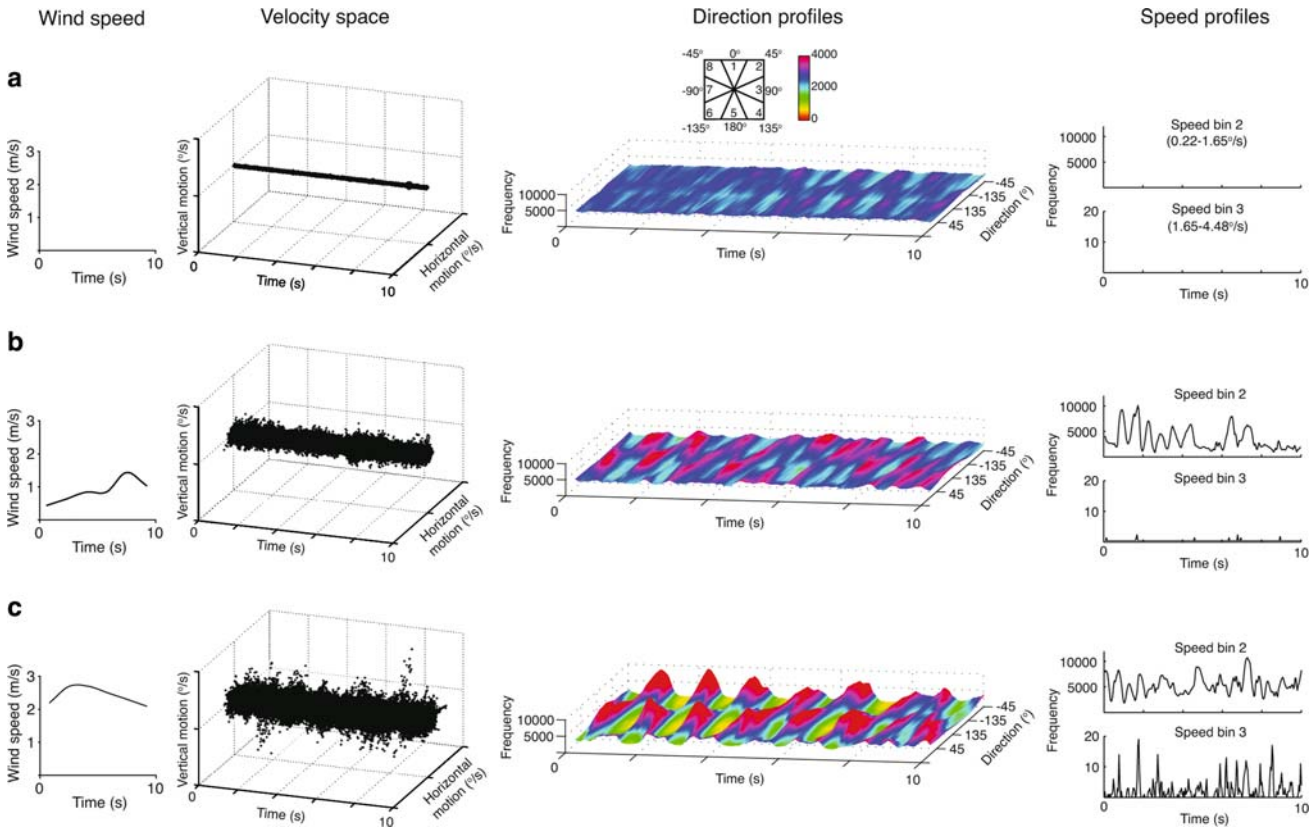

Fig. 4 Image motion caused by wind blown plants varies as a function of the prevailing wind conditions, illustrated here over 10 s samples for Site 1 (*Acacia longifolia*) in conditions of **a** no wind, **b** moderate wind and **c** strong wind. A change in prevailing wind modified the distribution of image motion as shown in velocity space, and as separate vector quantities of motion direction (*direction profiles*) and angular speed (*speed profiles*), summarised using non-overlapping direction and speed bins (see text for details). Direction bin frequencies greater than 4,000 are colour coded the same as 4,000

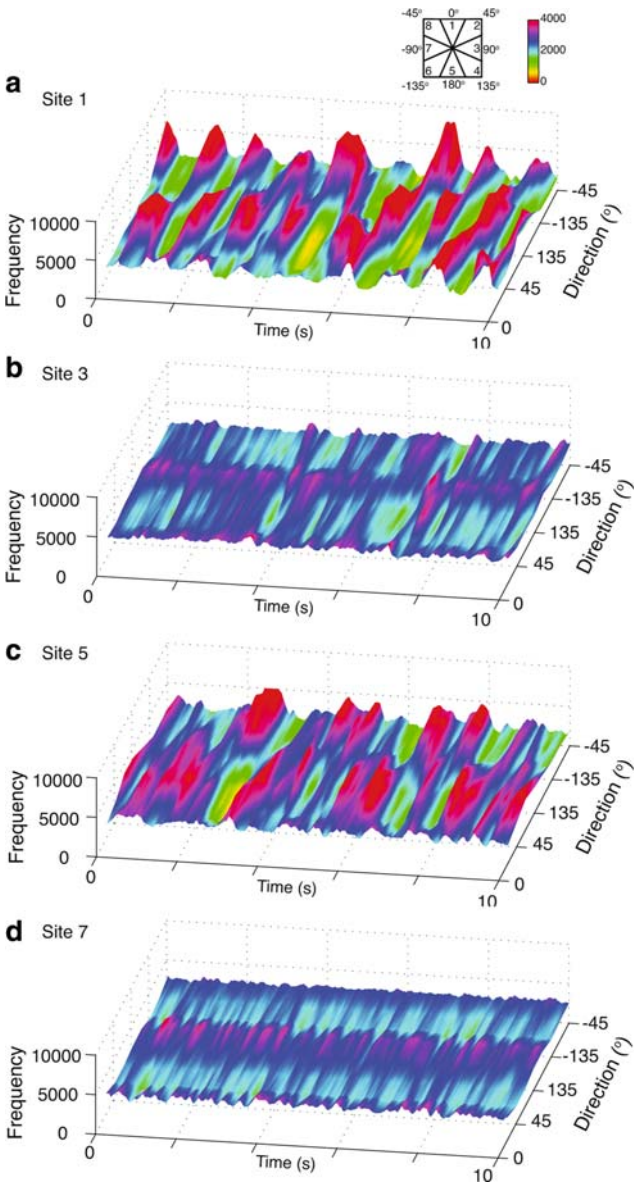

Fig. 5 Image motion environments vary between sites as shown in the direction profiles for four sites at wind speeds averaging 2.2 ms^{-1}: **a** site 1, *Acacia longifolia*, **b** site 3, *Lomandra longifolia*, **c** site 5, *Acacia sophorae*, and **d** site 8, *Casuarina glauca*. Direction profiles reflect distributions within 8 non-overlapping direction bins (frequencies greater than 4,000 are colour coded the same as 4,000)

speed profiles for bins 2 and higher (bins 2 and 3 shown) are at zero. Image motion in wind-still conditions thus featured low angular speed that is not dominated by any particular direction. A moderate increase in the prevailing wind resulted in higher velocities (Fig. 4b), and consequently, an increase in occupancy levels for speed bin 2. Furthermore, the direction profile now has more structure, and suggests a rhythmical temporal pattern of changing motion direction. The velocity distribution becomes broader yet when wind speed doubles (Fig. 4c). Angular speed increases, as shown by occupancy levels in speed bin 3, while the directionality and temporal structure of image motion has become even more pronounced.

The general pattern of results described in Fig. 4 reflected the trend across sites. There were, however, important differences between sites. We quantify these differences below in our regression models, but as an illustration we consider the degree of directionality observed at four different sites (Fig. 5). Under similar wind conditions, the direction profiles suggested that some sites are characterised by highly directional image motion (prominent peaks seen in Fig. 5a, c), while at other sites, the direction profiles show a less pronounced topography (Fig. 5b, d). Another important difference between sites was the spatial distribution of image motion, which likely depends on the specific vegetation structure (Fig. 6). Under calm conditions at sites 1 (*Acacia longifolia*) and 11 (*Westringia fruticosa*), angular speed is low (concentrated in speed bins 1 and 2) and has a relatively even distribution across the visual field (Fig. 6a). When wind increased at both sites, site 1 plants produced high-speed image motion in bins 3–5, but not at site 11 (Fig. 6b). Furthermore, when we partitioned the speed bin occupancies between different motion directions, we find that the stronger motion at site 1 is concentrated in diagonal motion directions (up/left, down/right; Fig. 7a). Conversely, increased wind conditions at site 11 generated a less directional distribution (Fig. 7b) with lower angular speeds (e.g., speed bins 4 and 5 in Fig. 6b).

Motion direction

The degree of image motion directionality varied across sites (Fig. 8a). The image motion at some sites was at times dominated by particular directions, as can be seen for sites 1, 5 and 7 (see also Fig. 5). Indeed some locations show high directionality even without strong wind (site 7; Fig. 8a). At sites 4, 8 and 12, however, image motion direction appeared more evenly distributed (M values close to zero). The directionality observed was strongly predicted by site and wind speed (Full model: $F_{23,840} = 226.6$, $P < 0.001$, Adjusted-$R^2 = 85.7\%$). We found differences between sites irrespective of wind speed ($F_{11,851} = 349.6$, $P < 0.001$; Fig. 8b), and a strong positive relationship with wind speed ($F_{1,851} = 581.7$, $P < 0.001$; Fig. 8b). A significant interaction term ($F_{11,840} = 10.5$, $P < 0.001$), however, suggested that the rate of increase in directionality varied across sites (Fig. 8b), as illustrated for sites 1 and 3 (Fig. 8c).

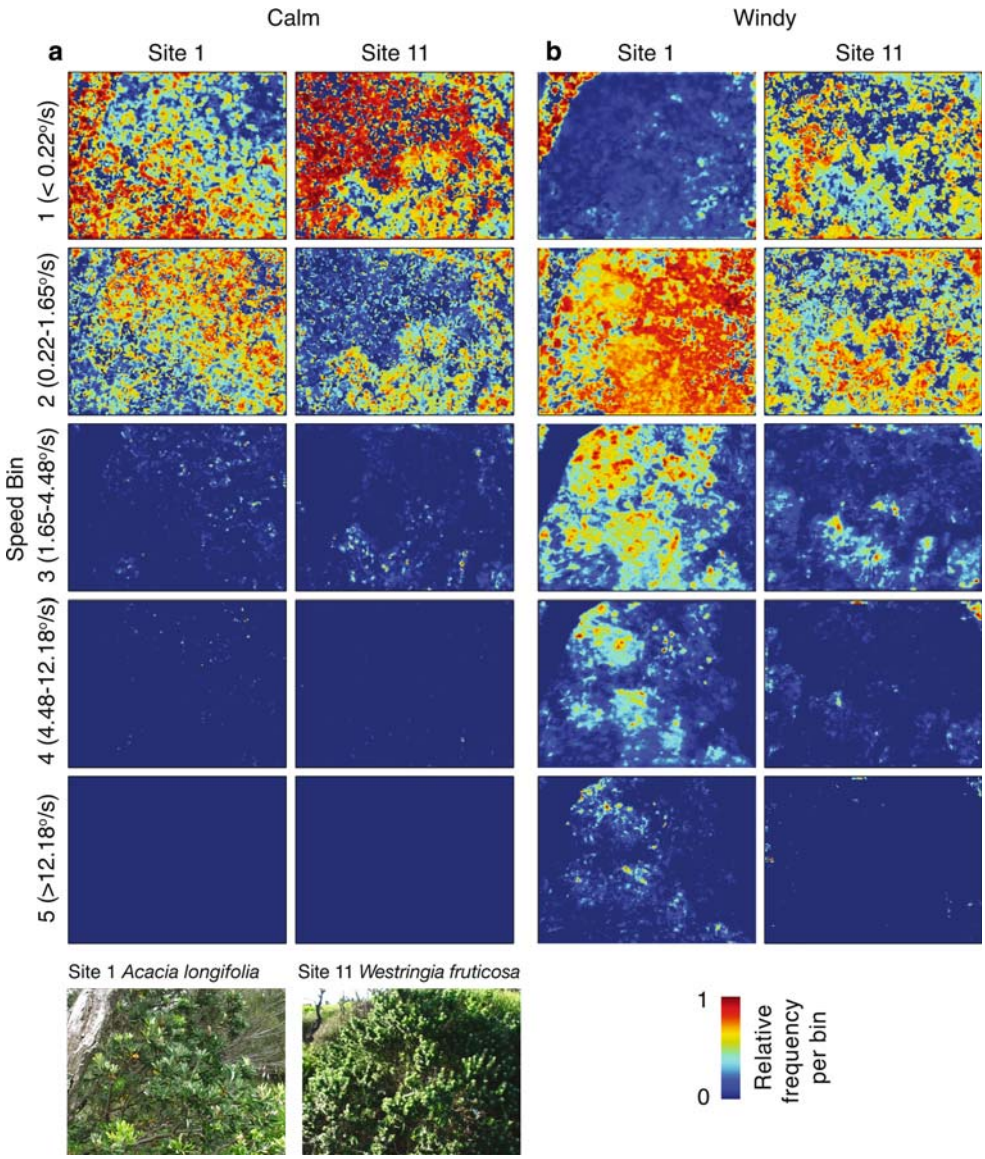

Fig. 6 The spatial distribution of angular speed at sites 1 (*Acacia longifolia*) and 11 (*Westringia fruticosa*) during **a** calm and **b** windy conditions, shown separately for each speed bin: from slow (*top row*) to fast (*bottom row*) angular speeds. The *bottom row* depicts a representative frame from each site. Values at each location represent the relative frequency of estimates for a 2 min filming session within each speed bin. Because bin occupancy differs between bins, cumulative frequencies are comparable in magnitude within a given row, but not between rows

Angular speed

At most sites, image motion was dominated by small angular speeds (high occupancies in bins 1 and 2; Fig. 9a). Frequencies varied across sites within each speed bin, and only a few sites generated image motion strong enough to register in higher speed bins (bins 4 and 5; Fig. 9a). Excluding sub-threshold values within each bin (see Methods), increased wind speed leads to higher levels of bin occupancy for all bins except, as expected, for the first (Fig. 9b). Both site and wind were found to be strong predictors of bin occupancy (Table 2), however, the interaction term was also significant in each case (Table 2), suggesting that the rate of increase is not uniform across sites.

Distance effects on perceived angular speed

Natural image motion distributions are the result of a complex mixture of different plant movements that are distributed in complicated patterns in depth. We were not in the position to quantify the depth-structure of our habitats (see c.f. Stürzl and Zeil 2007). So, for an initial assessment of how depth and movement distributions affect image motion distributions we modelled how perceived angular speed varies as a function of viewer distance (Fig. 10a) and movement speed (Fig. 10b; see "Materials and methods"). Plant movement of 20 cm/s at a distance of 50 ± 10 cm (mean ± SD) from the observer (red histogram in Fig. 10a), result in a broad distribution of angular speeds around 22°/s (red histogram on *y* axis of Fig. 10a).

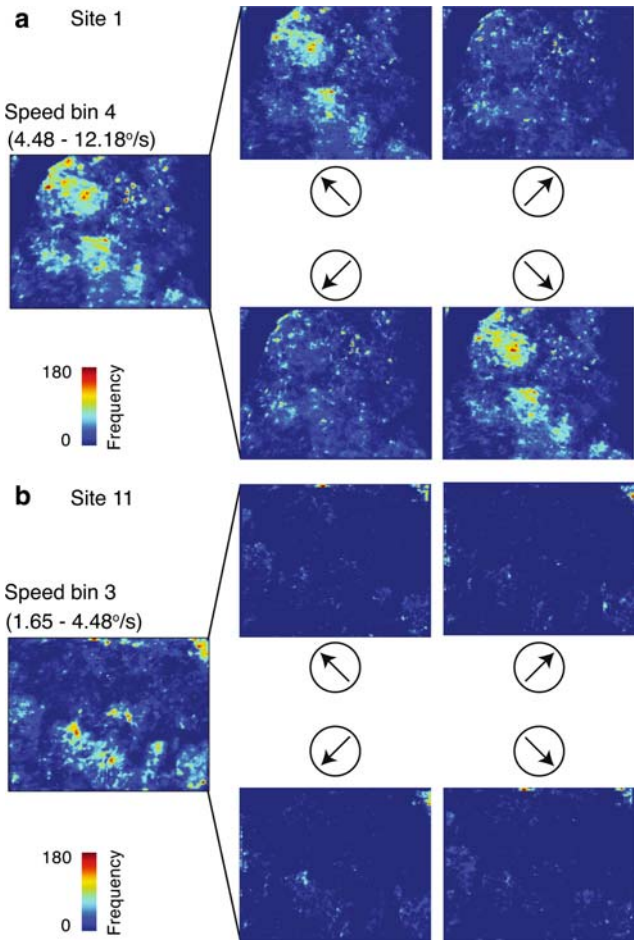

Fig. 7 The spatial distribution of motion for a single speed bin during windy conditions subdivided into 4 motion directions at **a** site 1 (*Acacia longifolia*) and **b** site 11 (*Westringia fruticosa*). Values at each location represent the cumulative frequency of estimates for a 2 min filming session

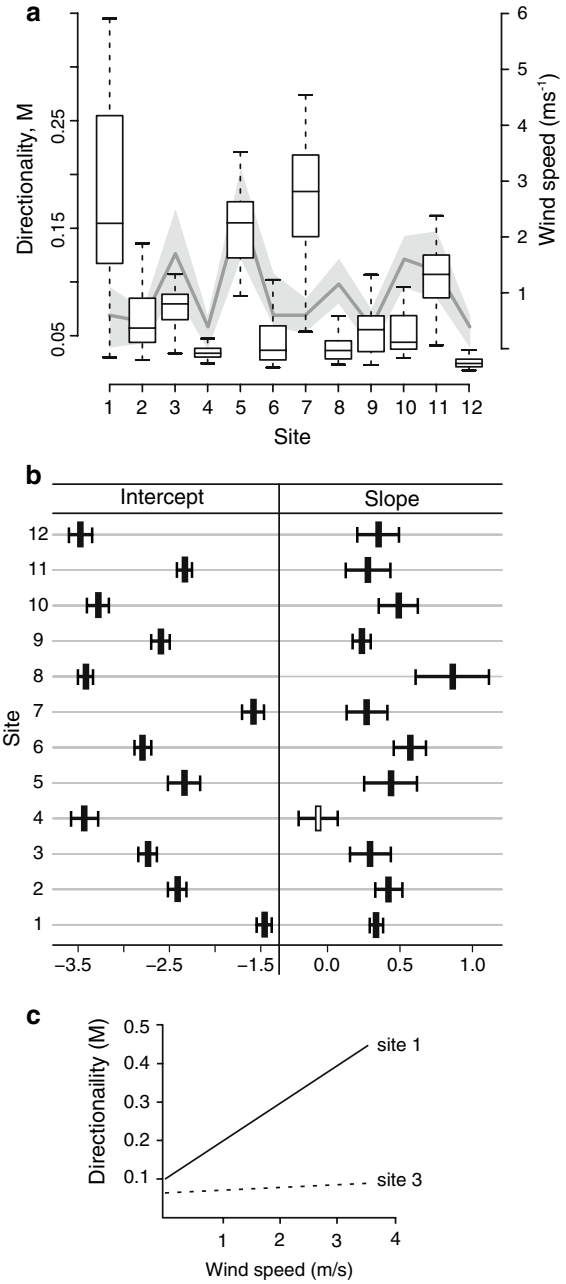

Fig. 8 **a** The directionality (*M*) of image motion at each site across the six filming sessions presented separately for each site. Values for *M* that approach 0 indicate an even distribution across the 8 sampling directions; an *M* equal to 1 indicates that all motion occurred in a single direction (see "Materials and methods" for further details). For each site, the *rectangular box* depicts the inter-quartile range and is dissected by the median. The *tails* represent the smallest and largest non-outliers. The *heavy grey line* underlying the directionality data depicts the median wind speed at each site, while the *shaded area* shows the inter-quartile range for wind speed. **b** Mean values (±SE) from 72 measurements per site (12/session) for the intercept and slope generated by generalized linear models comparing directionality (*M*) with wind speed (coefficients based on transformed values). The *unshaded box* for site 4 indicates the only non-significant estimate. **c** Regression lines for sites 1 and 3 back-transformed to the original scale

The same movement of plants further away at 200 ± 10 cm (blue histogram) generates much lower angular speeds and over a narrower range (about 6°/s; Fig. 10a). Increasing viewing distance, therefore, results in a shift to slower image motion speeds over a narrower range (red to blue histograms in Fig. 10a inset).

A change in movement speed at a given distance has a qualitatively similar effect (Fig. 10b). As above for a viewing distance of 50 ± 10 cm, a movement speed of 20 cm/s results in average image motion speeds of around 22°/s (dark green histogram on *y* axis of Fig. 10b). Plant movements of 10 cm/s at the same distance result in a narrower distribution of image motion around 11°/s (light green histogram on *y* axis of Fig. 10b). Increasing movement speed at a given distance, therefore, results in a shift to a wider range of faster image motion speeds (left to right in Fig. 10b inset).

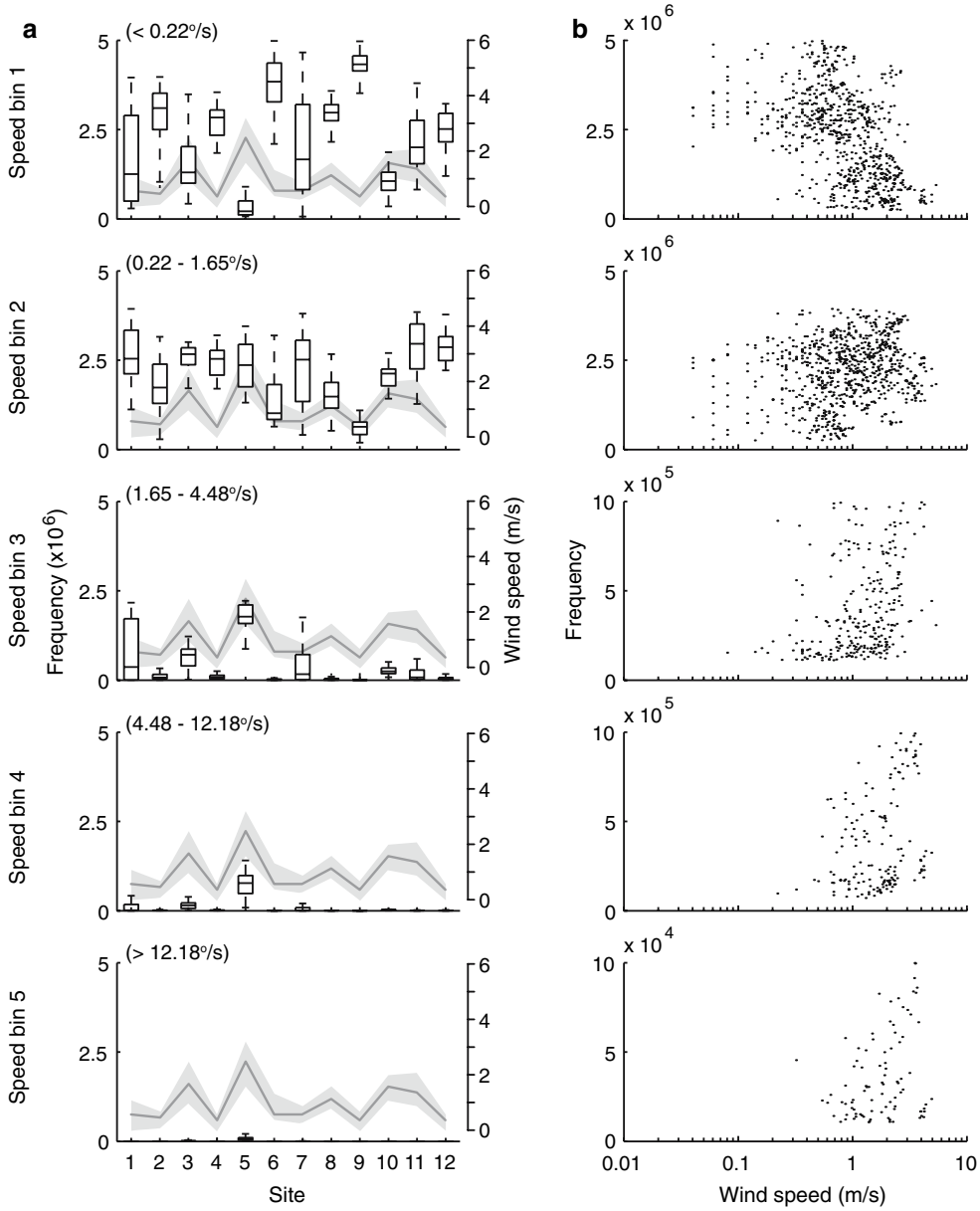

Fig. 9 Speed bin frequencies **a** by site and **b** as a function of wind speed. Separate plots are presented for each speed bin from slow (*top*) to fast (*bottom*) angular speeds. For each site in **a** the *rectangular box* depicts the inter-quartile range, dissected by the median, with the smallest and largest non-outliers defined by the tails. The *heavy grey line* underlying the directionality data depicts the median wind speed at each site, while the *shaded area* shows the inter-quartile range

As is apparent from Eq. (4) the critical value that predicts angular speed is in fact the ratio between viewer distance and movement speed (Fig. 10c). From this we can predict at what signaller-plant spacing patterns environmental motion noise will be at the same magnitude as the motion signals generated by a display. If the distribution of image motion speeds and the distance distributions of plants are known, the relationship shown in

Table 2 Analysis of deviance table from generalised linear models of angular speed

Speed	Site			Wind			Site × Wind		
bin	*F* value	*df*	*P* value	*F* value	*df*	*P* value	*F* value	*df*	*P* value
1	187.0	11,714	<0.0001	274.0	1,713	<0.0001	27.4	11,702	<0.0001
2	115.6	11,758	<0.0001	101.7	1,757	<0.0001	20.3	11,746	<0.0001
3	139.9	10,373	<0.0001	118.1	1,372	<0.0001	2.3	10,362	0.012
4	96.6	4,168	<0.0001	124.5	1,167	<0.0001	31.2	3,164	<0.0001
5	80.7	4,111	<0.0001	99.8	1,110	<0.0001	4.7	3,107	0.004

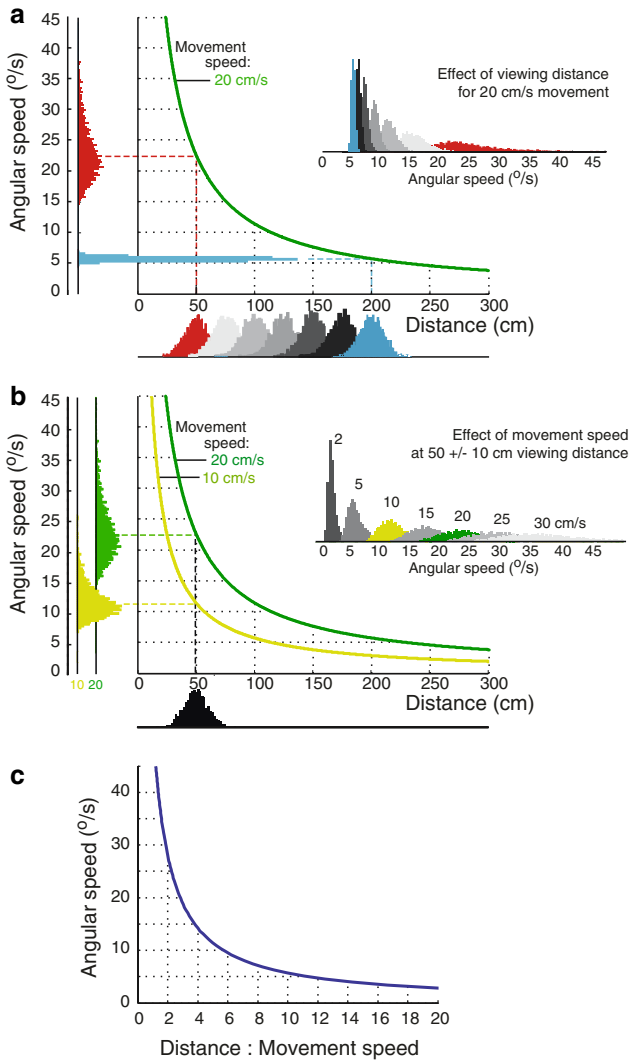

Fig. 10 Simulations quantifying the effect of viewing distance on motion signal distributions. **a** The relationship (*dark green curve*) between distance and angular speed for a movement speed of 20 cm/s. Mean angular speed generated by plants distributed around a mean distance of 50 ± 10 cm (*red histogram* on *x* axis) is around 22°/s (*red histogram* on *y* axis). Plants at 200 ± 10 cm (*blue histograms* on *x* and *y* axes) generate slower angular speeds over a narrower range. *Inset* angular speed distributions generated by 20 cm/s movements as viewing distance increases from 50 cm (*red histogram*), 75, 100, 125, 150, 175 to 200 cm (*blue histogram*). **b** The relationship between distance and angular speed for movement speeds of 20 cm/s (*dark green curve*) and 10 cm/s (*light green curve*). *Inset* angular speed distributions at a viewing distance of 50 ± 10 cm for movement speeds of 2, 5, 10, 15, 20, 25, 30 cm/s. **c** The relationship between angular speed and the ratio between viewing distance and movement speed for movement speeds larger or equal to movement amplitudes (i.e., ratio greater than 1)

Fig. 10c allows a prediction to be made on the signal movement speeds required for reliable detection. While this assumes that angular speed is used by the receiver visual system for segmenting signal and noise, it is apparent that the effective active space of a movement-based signal depends on the distance to surrounding vegetation (Fleishman 1988).

Discussion

Plant motion is expected to have contributed to the evolution of signal form and likely forces changes in signalling strategy under certain conditions (Fleishman 1988; Ord et al. 2007; Peters et al. 2007). In an effort to understand the type of environmental motion noise experienced by receivers, we have quantified the image motion generated by wind-blown plants at 12 sites in the coastal habitat of the Australian lizard *Amphibolurus muricatus.* Our analysis shows that each microhabitat represents a distinct image motion environment, as predicted by Fleishman (1986). We found that an increase in the prevailing wind had a profound effect on motion signal distributions (Fig. 4), although the exact nature differed across sites (Figs. 5, 6, 7). As wind increases, the image motion distribution becomes more directional (Figs. 4c, 8b), and angular speed increases (Figs. 4c, 9). The rate of change in directionality and angular speed with wind speed, however, was not the same at each site (Fig. 8b,c and Table 2 respectively), There were also site differences in the spatial distribution of image motion as wind changes (Figs. 6, 7). Furthermore, from first principles we show that the effect on angular speed of changing wind conditions depends critically on the distance distributions of plants and the viewing distance (Fig. 10): for a given movement speed there will be a wider range of angular speeds when viewed at close distances, becoming lower and narrower as observer-plant distance increases (Fig. 10b, c).

Implications for motion signal design

Theoretical models predict that environmental conditions at the time of signalling influence signal production and reception (e.g., Endler and Basolo 1998). The detection of movement-based signals requires the visual system to separate salient movements from motion noise in the environment. As Fleishman (1986) first demonstrated, movements that are atypical of plant motion are therefore likely to be particularly effective (see also Fleishman 1992; Bradbury and Vehrencamp 1998). What remains unclear, however, is the extent to which the spatiotemporal properties of signal and noise may overlap, and which motion characteristics reliably lead to segmentation.

To illustrate the potential masking effect of plant motion we overlaid footage of a signalling *A. muricatus* lizard on to wind blown plants at site 1 (*Acacia longifolia*) under varying wind conditions. We then compared the image

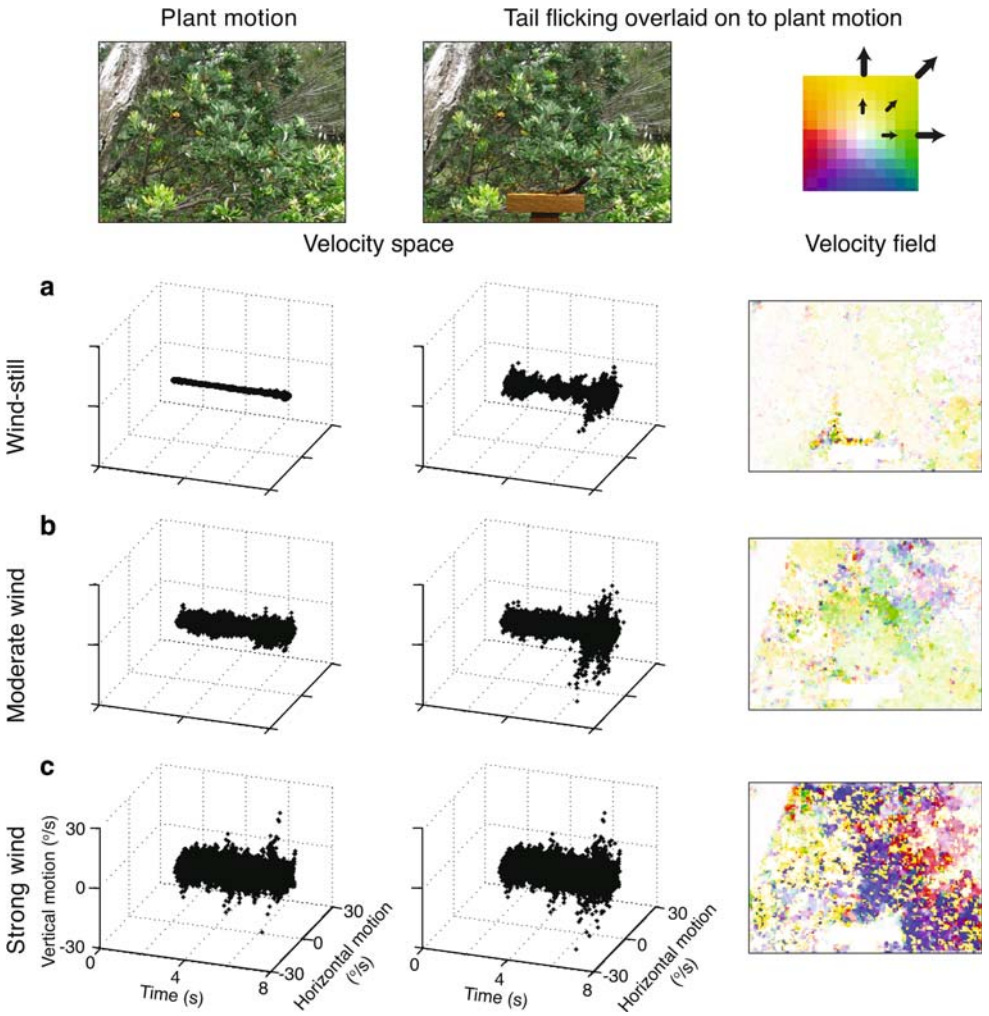

Fig. 11 An illustration of how an *A. muricatus* display is masked by wind-blown plants based on image motion distributions. Recordings of *Acacia longifolia* (site 1; *top*, *left column*) were selected in **a** wind-still, **b** moderate and **c** strong wind conditions (wind conditions as per Fig. 4). The resulting image motion distributions are shown in *velocity space* (*left column*). A display sequence from archival footage, with the background removed, was overlaid onto each of the plant sequences. The composite sequences (*top*, *middle column*) were then analysed in the same way. The resulting image motion distribution is also shown in *velocity space* (*middle column*). The presence of apparently faster motion speeds in the overlaid sequences for strong wind compared with moderate wind (**b**, **c** *middle column*) illustrates the interactive effect on motion detection mechanisms of movement in both the foreground and background. The *right hand column* depicts the velocity field for a portion of the tail-flick sequence (summed over 640 ms) showing the direction (*colour*) and speed (saturation) of image motion, according to the *colour code* shown on *top*, *right column* [from Zanker and Zeil (2005)]

motion distribution of these sequences with the same plant sequences without the signalling lizard (Fig. 11). In wind-still conditions, the animal's signal is highly conspicuous in velocity space. The introductory portion of the display features tail flicking, which generates stronger image motion values than the surrounding plants (Fig. 11a). As the wind becomes stronger, tail flicking becomes increasingly more difficult to distinguish from plant motion in both velocity space and in the velocity field (Fig. 11b, c). There is, however, a conspicuous portion of the velocity space profile in moderate conditions at the end of the sequence (Fig. 11b). This part of the display features vertical displacement of the lizard's upper body that is characteristic of a push up, as well as other motor patterns [see Peters and Ord (2003) for a description of the display]; in strong wind conditions, however, even these motor patterns will be difficult to identify on the basis of angular speeds and directionality alone. Figure 11 illustrates a surprising contradiction: the signal efficacy of the motor pattern *A. muricatus* uses for attracting the attention of receivers, tail flicking, may be more affected by variation in plant motion than the efficacy of the motor patterns that follow. Yet tail flicks do function to attract attention even though environmental motion in the habitat lengthens the time to detection (Peters 2008). Indeed, to increase the probability of detection these lizards tail flick intermittently

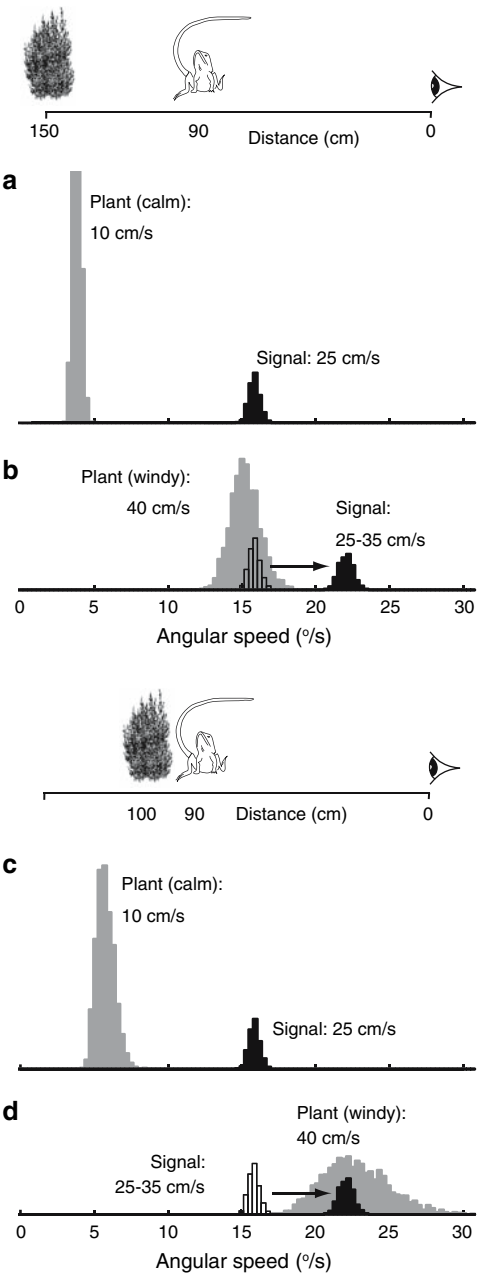

Fig. 12 Schematic diagram to illustrate how signal conspicuousness is influenced by the distance to background vegetation. **a** The image motion speed distribution of an animal signalling at a viewing distance of 90 ± 2 cm with a movement speed of 25 cm/s is clearly separated from that produced by a plant at a viewing distance of 150 ± 10 cm and moving at 10 cm/s. **b** A fourfold increase in plant movement speeds at that distance would swamp the signal. However, a small increase in display speed (to 35 cm/s) would ensure sufficient contrast to be detectable against the background plant motion. The outcome would be quite different if the plant were closer to the signaller, at a viewing distance of 100 ± 10 cm. **c** In calm conditions, the image motion of the animal signal and of the plant will remain well separated. **d** A fourfold change in plant motion speed at the closer viewing distance, however, will generate faster and broader image motion speeds. Consequently, the image motion caused by the faster display (35 cm/s) will be swamped by plant image motion. The animal signal speeds used in this illustration are based on estimates from *A. muricatus* tail-flicks, and represent the typical (25 cm/s) and upper range (35 cm/s) of values for tail tip displacement over time. The change in plant speed is also within the natural range of some plants (e.g., *Lomandra longifolia*)

over a longer period of time in windy conditions presumably in order to compensate for greater plant motion (Peters et al. 2007).

From a signal evolution perspective it is important to consider why these lizards lengthen signal duration rather than increasing signal speed, which seems to be the strategy used by other lizards (Fleishman 1988; Ord et al. 2007). Although there are likely to be multiple factors contributing to differences in signalling strategy, our current analysis suggests that variation in environmental image motion may have contributed to this divergence (Fig. 12). Simple simulations show that the geometry of the plant habitat can significantly influence the likelihood of signal detection based on perceived speed differences. Signalling on tree trunks in closed or open-canopy forests [as *Anolis cristatellus* and *Anolis gundlachi* do; Fleishman et al. (1997)] likely increases the spatial separation between the point of display and the nearest wind-blown plant. In calm conditions, the angular speed of an animal's signal will, therefore, be much higher than that of background plants (Fig. 12a). If stronger winds generated a four-fold increase in plant image motion (Fig. 12b), the animal would need only a moderate increase in display speed (from 25 to 35 cm/s) to overcome this background motion (Fig. 12b). In contrast, the populations of *A. muricatus* we study inhabit coastal heath that is dominated by low-lying shrubs. Signalling by these lizards is more likely to occur nestled within surrounding plants, such that the display and plant motion lie in similar depth planes (Fig. 12c). In calm conditions, the image motion generated by the animal signal and by plants will remain well separated despite the closer distance of the plants (see also Fig. 11a). Because of the close distance, however, a four-fold increase in plant movement speed has a much stronger effect on the resulting plant image motion speeds (Fig. 12d). Consequently, the image motion caused by the faster display speed (35 cm/s) will be swamped by plant image motion. As suggested by Fleishman (1988), it is likely to be very difficult to achieve speeds fast enough to exceed plant motion when both are performed close to the observer. Indeed, for the signal modelled here to achieve higher angular speeds than the plant background would require display speeds of approximately 50 cm/s that are well above those measured for *A. muricatus*. It may be that biomechanical and/or energetic constraints have prevented display speed adjustments being used to compensate for adverse environmental conditions. We suggest that *A. muricatus* evolved longer duration intermittent signalling

as an alternative strategy to deal with increased environmental motion (Peters et al. 2007).

This consideration also highlights the problem faced by the receivers' visual system in detecting the tail flick signal. Given the likelihood that the image motion distribution produced by flicking overlaps with that produced by wind blown plants, alternative mechanisms to speed differences are required to segment the signal. We know very little about the way motion sensitive neurons respond to plant motion and the degree to which they habituate to it (Fleishman 1986). The complicated patterns of motion distributions found in this study suggest that habituation may not be sufficient to isolate the signal. Clearly, the detection of a motion signal against the background of plant motion represents a figure-ground segmentation problem as Hailman (1977) suggested, which will need to be explored in more detail in future work. Possible segmentation mechanisms include phase differences between the figure and ground movement (Egelhaaf 1985; Lee and Blake 1999), coherent differences in reversals of motion direction (Lee and Blake 1999; Kandil and Fahle 2004) and motion onsets that generate large transients in the response of visual neurons [e.g., Ibbotson and Clifford (2001)].

In summary, we have quantified the image motion environments of a selected vertebrate species. The differences in image motion that we describe are likely to contribute to variation in signal efficacy as a function of display location and environmental conditions. In view of the interaction between plant mechanics and the variable layout of microhabitats, it will be difficult to predict image motion from first principles. The movement-based displays of animals, as well as the movement of plants at the time of signalling must be measured if we are to understand in detail the task facing receiver visual systems. We suggest, therefore, that movement-based signals may reveal the same type of habitat specific variation that we see for signals and neural processing mechanisms from other modalities.

Acknowledgments We thank the Edith and Joy London Foundation for hosting us during data collection, particularly the support provided by Robin and Steven Teding van Berkout. Thanks also to Waltraud Pix for assistance with identifying plant species, Nicole Carey for mathematical advice. We thank Leo Fleishman and an anonymous referee whose constructive comments greatly improved this paper. This work was funded by the Australian Research Council. JMH and JZ acknowledge support from the ARC Centre of Excellence Program.

References

Boeddeker N, Lindemann J, Egelhaaf M, Zeil J (2005) Responses of blowfly motion-sensitive neurons ro reconstructed optic flow along outdoor flight paths. J Comp Physiol A 191:1143–1155

Bradbury JW, Vehrencamp SL (1998) Principles of animal communication. Sinauer Associates Inc., Sunderland

Brumm H, Voss K, Köllmer I, Todt D (2004) Acoustic communication in noise: regulation of call characteristics in a new world monkey. J Exp Biol 207:443–448

Cocroft RB, Rodriguez R (2005) The behavioural ecology of insect vibrational communication. Bioscience 55:323–334

Cogger HG (1996) Reptiles and amphibians of Australia. Reed Books, Port Melbourne

Costermans L (2005) Native trees and shrubs of south-eastern Australia. Reed New Holland, Sydney

Cynx J, Lewis R, Tavel B, Tse H (1998) Amplitude regulation of vocalizations in noise by a songbird, *Taeniopygia guttata*. Anim Behav 56:107–113

Dusenbery DB (1992) Sensory ecology: how organisms acquire and respond to information. W.H. Freeman and Company, New York

Eckert MP, Zeil J (2001) Towards an ecology of motion vision. In: Zanker JM, Zeil J (eds) Motion vision: computational, neural, and ecological constraints. Springer, Berlin, pp 333–369

Egelhaaf M (1985) On the neuronal basis of figure-ground discrimination by relative motion in the visual system of the fly. I: Behavioural constraints imposed on the neuronal network and the role of the optomotor system. Biol Cybern 52:123–140

Egelhaaf M, Borst A, Reichardt W (1989) Computational structure of a biological motion-detection system as revealed by local detector analysis in the fly's nervous system. J Opt Soc Am A 6:1070–1087

Elias D, Land B, Mason A, Hoy R (2006) Measuring and quantifying dynamic visual signals in jumping spiders. J Comp Physiol A 192:785–797

Endler JA (1993) The color of light in forests and its implications. Ecol Monogr 63:1–27

Endler JA, Basolo AL (1998) Sensory ecology, receiver biases and sexual selection. Trends Ecol Evol 13:415–420

Endler JA, Thery M (1996) Interacting effects of lek placement, display behavior, ambient light, and color patterns in three neotropical forest-dwelling birds. Am Nat 148:421–452

Fleishman LJ (1986) Motion detection in the presence or absence of background motion in an *Anolis* lizard. J Comp Physiol A 159:711–720

Fleishman LJ (1988) Sensory and environmental influences on display form in *Anolis auratus*, a grass anole of Panama. Behav Ecol Sociobiol 22:309–316

Fleishman LJ (1992) The influence of the sensory system and the environment on motion patterns in the visual displays of anoline lizards and other vetebrates. Am Nat 139(Supplement):S36–S61

Fleishman LJ, Bowman M, Saunders D, Miller WE, Rury MJ, Loew ER (1997) The visual ecology of Puerto Rican anoline lizards: Habitat light and spectral sensitivity. J Comp Physiol A 181:446–460

Greenfield MD (1988) Interspecific acoustic interactions among katydids *Neoconocephalus*: inhibition induces shifts in diel periodicity. Anim Behav 36:684–695

Hailman JP (1977) Optical signals: animal communication and light. Indiana University Press, Bloomington

Hannah P, Palutikof J, Quine C (1995) Predicting windspeeds for forest areas in complex terrain. In: Coutts M, Grace J (eds) Wind and trees. Cambridge University Press, Cambridge, pp 113–129

Hardwick RJ (2001) Nature's larder: a field guide to the native plants of the NSW south coast. Homosapien Books, Jerrabomberra

Hayes A, Huntly N (2005) Effects of wind on the behaviour and call transmission of pikas (*Ochotona princeps*). J Mammal 86:974–981

Ibbotson M, Clifford CWG (2001) Characterising the temporal delay filters of biological motion detectors. Vision Res 41:2311–2323

Kandil F, Fahle M (2004) Figure-ground segregation can rely on differences in motion direction. Vision Res 44:3177–3182
Lee S-H, Blake R (1999) Visual form created solely from temporal structure. Science 284:1165–1168
Lengagne T, Slater P (2002) The effects of rain on acoustic communication: tawny owls have a good reason for calling less in wet weather. Proc R Soc Lond B 269:2121–2125
Lythgoe JN (1979) The ecology of vision. Oxford University Press, Oxford
Ord T, Peters R, Clucas B, Stamps J (2007) Lizards speed up visual displays in noisy motion habitats. Proc R Soc Lond B 274:1057–1062
Peters R (2008) Environmental motion delays the detection of movement-based signals. Biol Lett 4:2–5
Peters R, Hemmi J, Zeil J (2007) Signalling against the wind: modifying motion signal structure in response to increased noise. Curr Biol 17:1231–1234
Peters RA, Clifford CWG, Evans CS (2002) Measuring the structure of dynamic visual signals. Anim Behav 64:131–146
Peters RA, Evans CS (2003) Design of the jacky dragon visual display: signal and noise characteristics in a complex moving environment. J Comp Physiol A 189:447–459
Peters RA, Ord TJ (2003) Display response of the jacky dragon, *Amphibolurus muricatus* (Lacertilia: Agamidae), to intruders: a semi-markovian process. Austral Ecol 28:499–506
Potash L (1972) Noise-induced changes in calls of the japanese quail. Psychon Sci 26:252–254
R Development Core Team (2006) R: a language for statistical computing, Vienna. R Foundation for Statistical Computing, Vienna
Reichardt W, Egelhaaf M (1988) Properties of individual movement detectors as derived from behavioural experiments on the visual system of the fly. Biol Cybern 58:287–294
Slabbekoorn H, den Boer-Visser A (2006) Cities change the songs of birds. Curr Biol 16:2326–2331
Slabbekoorn H, Peet M (2003) Birds sing at a higher pitch in urban noise. Nature 424:267
Slabbekoorn H, Smith T (2002) Habitat-dependent song divergence in the little greenbul: an analysis of environmental selection pressures on acoustic signals. Evolution 56:1849–1858
Stürzl W, Zeil J (2007) Depth, contrast and view-based homing in outdoor scenes. Biol Cybern 96:519–531
Sun J, Narins PM (2005) Anthropogenic sounds differentially affect amphibian call rate. Biol Conserv 121:419–427
Wiley RH, Richards DG (1982) Adaptations for acoustic communication in birds: sound transmission and signal detection. In: Kroodsma DE, Miller EH (eds) Acoustic communication in birds volume 1: Production, perception, and design features of sounds. Academic Press, New York, pp 131–181
Witte K, Farris H, Ryan MJ, Wilczynski W (2005) How cricket frog females deal with a noisy world: habitat-related differences in auditory tuning. Behav Ecol 16:571–579
Wood C (1995) Understanding wind forces on trees. In: Coutts M, Grace J (eds) Wind and trees. Cambridge University Press, Cambridge, pp 133–164
Zanker JM, Zeil J (2005) Movement-induced motion signal distributions in outdoor scenes. Network-Comp Neural 16:357–376
Zeil J, Zanker JM (1997) A glimpse into crabworld. Vision Res 37:3417–3426